

Observational constraints on disk galaxy formation

D. Syer, Shude Mao, and H.J. Mo ^{*}

Max-Planck-Institut für Astrophysik Karl-Schwarzschild-Strasse 1, 85748 Garching, Germany

Accepted Received; in original form

ABSTRACT

We use data from the literature to constrain theoretical models of galaxy formation. We show how to calculate the dimensionless spin parameter λ of the halos of disk galaxies and we compare the distribution of λ with that observed in cosmological N -body simulations. The agreement is excellent, which provides strong support for the hierarchical picture of galaxy formation. Assuming only that the radial surface density distribution of disks is exponential, we estimate crudely the maximum-disk mass-to-light ratio in the I -band and obtain $\langle \Upsilon_I \rangle \lesssim 3.56h$, for a Hubble constant of $100h \text{ km s}^{-1} \text{ Mpc}^{-1}$. We discuss this result and its limitations in relation to other independent determinations of Υ_I . We also define a dimensionless form of the Tully-Fisher relation, and use it to derive a value of the baryon fraction in disk galaxies. For galaxies with circular velocity $v_m > 100 \text{ km s}^{-1}$, the median value is $m_d = 0.086(\Upsilon_I/3.56h)$. Assuming that the gas fraction in galactic halos is at most as large as that in clusters, we also conclude that $\langle \Upsilon_I \rangle \lesssim 2.48h^{-1/2}$.

Key words: galaxies: disk - galaxies: structure - cosmology: theory - dark matter

1 INTRODUCTION

The fact that the rotation curves of spiral galaxies are rather flat is usually taken to imply the presence of an extended halo of dark matter (e.g. Freeman 1970, Persic & Salucci 1991). If such dark matter exists, then hierarchical models of galaxy formation (White & Rees 1978) are a natural consequence of gravitational instability. In these models the standard picture of disk formation is that gas, which is initially distributed in the same way as the dark matter, cools and settles into rotationally supported disks at the centres of dark matter halos (Fall & Efstathiou 1980).

Dalcanton, Spergel & Summers (1997), and Mo, Mao & White (1998) (MMW) have shown recently that such a picture can reproduce some of the broad properties of observed disk galaxies. In particular they show that the Tully-Fisher relation (Tully & Fisher 1977) can be understood very simply. However, as was pointed out by Courteau & Rix (1997), the Tully-Fisher relation is incompatible with the maximum-disk hypothesis (Carignan & Freeman 1985) if disk galaxies have universal mass-to-light ratios (de Jong 1996).

Great interest in the Tully-Fisher relation as a distance indicator (Giovanelli *et al.* 1997 and references therein) has led to many observations of disk galaxies, and large samples are now available (e.g. Mathewson & Ford 1996; Courteau 1996, 1997). In this paper, we examine the observational

constraints which can be placed on the standard picture of disk formation.

In the next section we review the properties of exponential disks and the scenario of disk formation. We start from the standard assumption that the disk mass-to-light ratio Υ is universal (or at least does not vary strongly with surface brightness), and calculate various components from observable quantities. In Section 3 we describe the observations of disk galaxies. In Section 4 we show the results of applying the theory of Section 2 to the data. In Section 5 we discuss the implications of our results and draw conclusions. In particular, Section 5.1 is devoted to a discussion of independent determinations of Υ .

2 DISK FORMATION

2.1 Exponential disks

The luminous disks of spiral galaxies are commonly modelled by an exponential surface brightness distribution:

$$\mu(R) = \frac{L_d}{2\pi R_d^2} \exp(-R/R_d) \quad (1)$$

where R is the usual cylindrical radius, R_d is the exponential scalelength, and L_d is the total luminosity of the disk. Here we collect some notation and a number of useful results relating to exponential disks.

The disk has a mass M_d , and a mass-to-light ratio Υ in solar units. Thus the surface mass density of the disk is

* E-mail: (syer, smao, hom)@mpa-garching.mpg.de

$$\Sigma(R) = \mu(R)\Upsilon = \frac{M_d}{2\pi R_d^2} \exp(-R/R_d). \quad (2)$$

The gravitational potential in the disk Φ is conveniently decomposed into contributions from the disk and a halo:

$$\Phi = \Phi_d + \Phi_h. \quad (3)$$

(We use the subscripts ‘d’ for ‘disk’, and ‘h’ for ‘halo’ throughout.) We assume for the present purposes that the halo is spherical, and usually we think of it as being composed of dark matter, but it may also contain a stellar component (e.g. the ‘bulge’ of an earlier type spiral).

The speed of test particles on circular orbits v_c as a function of R is given by

$$v_c^2(R) = -R \frac{\partial \Phi}{\partial R}. \quad (4)$$

We shall refer to $v_c(R)$ as the rotation curve of the system. The rotation curve as measured in HI (apart from small contributions from turbulent motion) is thought to be a good measure of the true rotation curve as long as the system is axisymmetric.

We characterise the self gravity of the disc through the the dimensionless quantity

$$\epsilon_m = \frac{v_m}{(GM_d/R_d)^{1/2}}, \quad (5)$$

where v_m is the maximum value of v_c , and G is the gravitational constant. The rotation curve of an isolated exponential disk ($\Phi_h = 0$) is given by Freeman (1970). An isolated disk has $\epsilon_m = \epsilon_d \approx 0.63$ and a disk embedded in a halo has $\epsilon_m > \epsilon_d$.

The directly observable quantity corresponding to ϵ_m is

$$\epsilon_l = \frac{v_m}{(GL_d/R_d)^{1/2}}, \quad (6)$$

which is related to ϵ_m by

$$\epsilon_l = \epsilon_m \Upsilon^{1/2}. \quad (7)$$

The quantity ϵ_l^2 has the units of a mass-to-light ratio, and indeed it is a measure of the *total* mass (including dark matter halo) contributing to the rotation curve. Let us define a quantity

$$\Upsilon^{\text{tot}}(R) = \frac{v_c^2(R)R}{GL(R)}, \quad (8)$$

which measures the total mass-to-light ratio as a function of radius. For an isolated disk it is a constant ($= \Upsilon$) and with an extended dark halo it increases with radius. The maximum rotation velocity in general occurs at $R = R_{\text{max}} > R_d$, and the luminosity enclosed is $L_{\text{max}} < L_d$, hence $\epsilon_l^2 < \Upsilon^{\text{tot}}(R_{\text{max}})$. For an isolated disk $R_{\text{max}} = 2.2R_d$ and $L_{\text{max}} = 0.65L_d$, so $\Upsilon = \Upsilon^{\text{tot}}(R_{\text{max}}) = 3.4\epsilon_l^2$.

2.2 Disk Formation Model

Here we reproduce a simple model where the dark matter halo is assumed to be a singular isothermal sphere and disc self-gravity is neglected (cf MMW). In this model, the disk scale length is

$$R_d = \frac{1}{\sqrt{2}} \lambda R_h \quad (9)$$

where λ is the dimensionless spin parameter, R_h is the virial radius of the halo. The halo properties are given by

$$M_h = \frac{v_h^2 R_h}{G}, \quad R_h = \chi \frac{v_h}{H_0} \quad (10)$$

where M_h is the mass and v_h the circular velocity of the halo, $H_0 = 100 h \text{ km s}^{-1} \text{ Mpc}^{-1}$ is the Hubble constant and χ is a dimensionless constant. For discs assembled at redshift z , MMW argue that $\chi \approx 0.1 H_0 / H(z)$, where $H(z)$ is the Hubble constant at z . We can treat χ as an adjustable parameter and derive its value from observational data. Whenever we need a numerical value for χ we use the one derived in Section 4.2 ($\chi = 0.049$). The maximum rotation velocity of the disk is $v_m \approx v_h$.

When more realistic halo profiles are used and disc self-gravity is taken into account, the relation between R_d and v_h is slightly modified from that given by equations (9) and (10) (see MMW for details). The constant part of such modifications can be taken into account by the constant χ . For simplicity, we will ignore all high order effects.

The disk central surface density is given by

$$\Sigma_0 = \frac{m_d M_h}{2\pi R_d^2} \quad (11)$$

where m_d is the fraction of halo mass that settles into the disk. We now define a dimensionless ratio of observables

$$\begin{aligned} \lambda_m^2 &\equiv \frac{H_0}{h} \frac{v_m}{\pi G \mu_0} \frac{1}{\Upsilon} \\ &= 1.47 \times 10^{-2} \left(\frac{v_m}{200 \text{ km s}^{-1}} \right) \left(\frac{100 L_\odot \text{ pc}^{-2}}{\mu_0} \right) \end{aligned} \quad (12)$$

where $\mu_0 = \Sigma_0 / \Upsilon$ is the central surface brightness. Defining also the structural parameter

$$a_m \equiv \frac{m_d h}{\Upsilon} \frac{1}{\chi}, \quad (13)$$

we combine equations (9-13) to obtain an expression for λ :

$$\lambda^2 = \lambda_m^2 a_m. \quad (14)$$

From equations (5), (9) and (10) we find that

$$\epsilon_m^2 = \frac{1}{\sqrt{2}} \frac{\lambda}{m_d} \quad (15)$$

which is a dimensionless description of disk formation: the smaller the spin parameter λ , the more concentrated the disk, and the more self-gravitating it is (smaller ϵ_m). We can write equation (15) in terms of observables as

$$\epsilon_l^2 h^{-1} = \frac{1}{\sqrt{2} \chi} \frac{\lambda_m}{a_m^{1/2}}. \quad (16)$$

Equation (16) is just the dimensionless form of the Tully-Fisher relation. To see this we write the Tully-Fisher relation as

$$H_0^2 L = A v_m^3, \quad (17)$$

where the value of A can be derived from equations (9-11):

$$A = a_m \chi^2 \frac{H_0}{hG}. \quad (18)$$

Equations (16) and (17) both relate observable quantities via the same constant of proportionality (i.e. $a_m \chi^2$), and hence (16) is a dimensionless form of the Tully-Fisher relation (17).

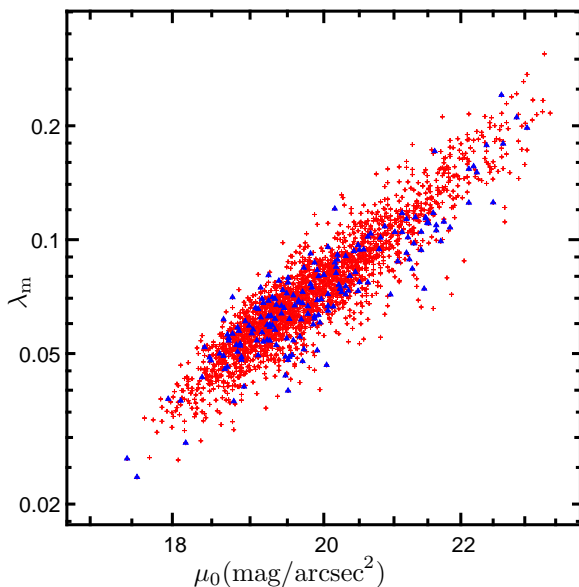


Figure 1. The relationship between λ_m and the central surface brightness μ_0 (in the I band) of the sample of spiral galaxies of Mathewson & Ford (1996). Barred galaxies are shown as triangles.

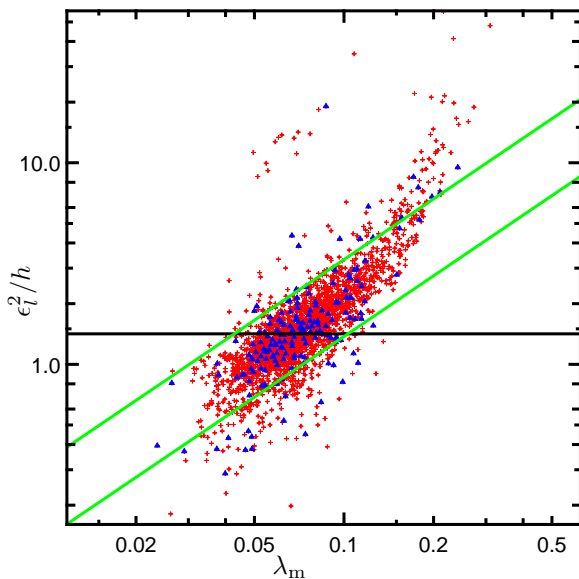


Figure 2. The dimensionless Tully-Fisher relation (equation 16) for the MF data set. On this plot, a fixed value of ϵ_m corresponds to a horizontal line with amplitude $\epsilon_m^2(\Upsilon_I h^{-1})$. The horizontal solid line shows the value of ϵ_m for a self-gravitating disk ($\epsilon_m = 0.63$) with $\Upsilon_I = 3.56h$. The two dashed lines contain 90% of the data with slope and scatter predicted by the Tully-Fisher relation, within the framework of MMW (see text). Barred galaxies are shown as triangles.

An important parameter in the above model is the dimensionless spin λ of the system before disk formation. In the hierarchical model of galaxy formation, much is known about its expected value and distribution (Cole & Lacey 1996, Warren *et al.* 1992, Lemson & Kauffmann 1998). We can use equations (14) and (16) to write

$$\lambda = \frac{1}{\sqrt{2}\chi} \frac{\lambda_m^2 h}{\epsilon_l^2} \quad (19)$$

the right hand side of which contains *only* observable quantities (and the constant χ). Thus, this equation can be used to derive the distribution of λ from observations once the value of χ is fixed (see Section 4.2).

3 OBSERVATIONS

To compare theory with observations we use the dataset of Mathewson & Ford (1996) (MF) which has rotation velocities and I-band photometry for a sample of nearly 2500 Southern spiral galaxies selected randomly from the ESO-Uppsala catalogue (Lauberts 1982). The majority are relatively late types: of those 2275 for which Hubble types are given, 1055 are Sc or Sbc; 814 are Sb; and 5 are Sa. We convert the published photometric quantities to R_d and the central surface brightness μ_0 by assuming an exponential profile. Details are given in an Appendix.

The observed Tully-Fisher relation (Giovanelli *et al.* 1997; Shanks 1997):

$$M_I - 5 \log h = -(21.00 \pm 0.02) - (7.68 \pm 0.13)(\log W - 2.5), \quad (20)$$

where W is the inclination-corrected width of the HI line profile. The MF data has a Tully-Fisher relation which is consistent with this, albeit with larger scatter than in more carefully selected samples.

The maximum of the rotation curve v_m is given by $v_m = W/2$. Figure 1 shows the relationship between λ_m and the central surface brightness μ_0 of the MF data set. The correlation is expected, since halos with smaller λ should form more compact disks with higher Σ_0 . This figure illustrates that λ and μ_0 are almost interchangeable, despite the fact that in principle the correlation could have been washed out by scatter in v_m . The tight correlation between λ_m and μ_0 therefore implies that the disk central surface brightness is determined mainly by halo spin parameter rather than by halo circular velocity, as is expected in the disk formation model (see §2.2). From equations (9)-(11) we see that the disk central surface density scales with v_h and λ as $\Sigma_0 \propto v_h/\lambda^2$. The dynamical range of v_h for disk galaxies is a factor of about 3, while that for λ^2 predicted for dark halos is a factor of about 15.

In Figure 2, we show ϵ_l as a function of λ_m for the MF data. The extra factor of h in the abscissa makes the plotted quantities independent of the Hubble constant. The figure reveals a marked correlation between ϵ_l and λ_m which corresponds to the dimensionless Tully-Fisher relation (equation 16). The slope is unity provided a_m is independent of λ_m . The figure shows that the slope is consistent with unity for the majority of galaxies. At the large λ_m end the observed ϵ_l is slightly higher than the model prediction. There appears to be a break in the slope of ϵ_l versus λ_m at $\lambda_m \approx 0.1$. According to the model in Section 2.2 a higher value of ϵ_l would mean that the combination $m_d h/\Upsilon$ is lower for low-surface-brightness galaxies. This would result from a lower star formation efficiency (hence higher Υ), as suggested by observations (e.g. McGaugh & de Blok 1997).

For a given λ_m , the scatter in ϵ_l is determined by the scatter in the Tully-Fisher amplitude A . In Figure 2, we overlay the predicted slope (i.e. unity, see equation 16) and

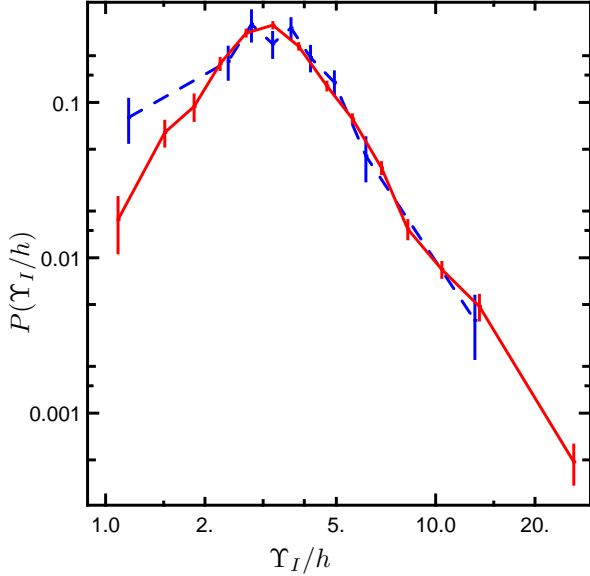


Figure 3. The distribution of Υ_I for the MF data, on the assumption that all disks are exponential and self-gravitating. The solid line is the whole sample, and the dashed line is for the barred subsample. The error bars are estimated using a standard bootstrap method.

scatter on top of the data points with the normalisation chosen to reproduce the observed median value of ϵ_l in the range $\lambda_m \in (.05, .06)$. The lines are derived from the 5% and 95% quartiles of A of the data—the equivalent scatter in A is a factor of ≈ 2.4 or 0.95 magnitudes. The predicted slope and scatter are consistent with the observed data points. Thus, the data are consistent with the assumption that the value of a_m is independent of λ_m for the majority of these galaxies. This is an important result, because it means that the total mass-to-light ratio, $M_h/L_d = \Upsilon/m_d \propto a_m^{-1}$, is a constant for the majority of galaxies. We will return to this point in the next section.

4 CONSTRAINING GALAXY FORMATION

In this Section, we use the observational data to constrain the disk model described in Section 2.2. We concentrate on the three most important parameters in the disk model: the mass-to-light ratios of disks, the spin parameters of halos, and the baryon fractions in disks.

4.1 Mass-to-light ratios

Assuming that the disks are exponential sets a limit on Υ_I : they should all have $\epsilon_m > 0.63$, the value for an isolated disk. Thus for each galaxy $\Upsilon_I \lesssim (\epsilon_l/0.63)^2$, which is a crude estimate of the maximum-disk mass-to-light ratio. Figure 3 shows the distribution of Υ_I calculated in this way for the MF data, and for the barred subset. In Figure 2 the solid horizontal line marks the median of ϵ_l in the data of Mathewson & Ford (1996). This corresponds to $\epsilon_m = 0.63$ for $\Upsilon_I = 3.56h$.

A conservative upper limit for the average disk galaxy would be $\langle \Upsilon_I \rangle < 3.56h$. This limit is also consistent with

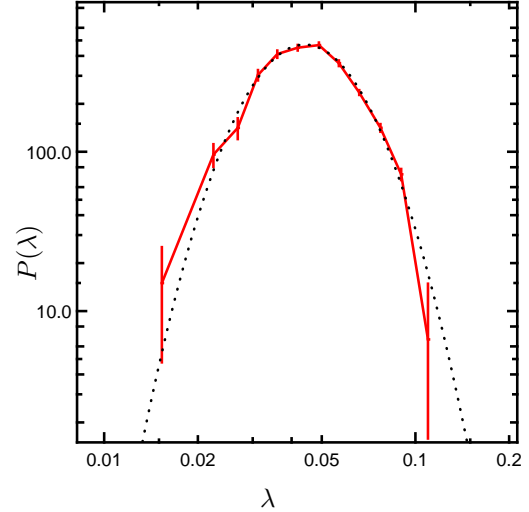


Figure 4. The distribution of λ for the MF data (solid line with error bars). The best fit to a log-normal distribution ($\bar{\lambda} = 0.05$, $\sigma = 0.36$) is shown as a dotted line. The error bars are estimated using a standard bootstrap method.

independent measurements of Υ_I (see Section 5.1 for details). However, since ϵ_l is higher for low surface brightness galaxies, a higher Υ_I is still allowed for these galaxies without violating the constraint $\epsilon_m > 0.63$. Similarly, for high surface brightness galaxies, a lower Υ_I is required to avoid violating the constraint $\epsilon_m > 0.63$. Note that if Υ_I were not universal, then the Tully-Fisher relation would require that $m_d \propto \Upsilon_I$. In the opposite case, if Υ_I were universal, a more stringent upper limit on Υ_I would be required, in order to accommodate high surface brightness galaxies.

4.2 Spin parameters

The distribution of λ can be determined from N -body simulations of hierarchical clustering, and is found to be log-normal with mean $\bar{\lambda} \approx 0.05$ and standard-deviation $\sigma \approx 0.5$ almost independent of cosmology (Lemson & Kauffmann 1998, Warren *et al.* 1992). If observations of disk galaxies are a fair sample of dark matter halos, then the distribution of λ_m should be closely related to the distribution of λ . The distribution of λ in the MF data (calculated from equation 19) is shown in Figure 4. The value of $\bar{\lambda}$ has been fixed at 0.05 by choosing $\chi = 0.049$. As discussed in Section 2.2, $\chi \approx 0.1H_0/H(z)$ for isothermal halos. Using more realistic halo profiles and taking into account disk self gravity reduces the value of R_d for a given v_m , which corresponds to a reduction of the value of χ . This value of χ found here is actually in good agreement with the detailed modelling of MMW.

The distribution is remarkably close to log-normal with $\sigma = 0.36 \pm 0.01$. The value of σ derived from the data is smaller than the value, $\sigma = 0.5$, given by N -body simulations of dark halos. The reason for this discrepancy may be due to the fact that the observational sample is biased against both low-surface brightness galaxies, which are associated with high-spin systems according to the disk model considered here, and early type spirals, which are associated with low-spin systems. The main effect of the selection function is to rule out galaxies below some threshold in sur-

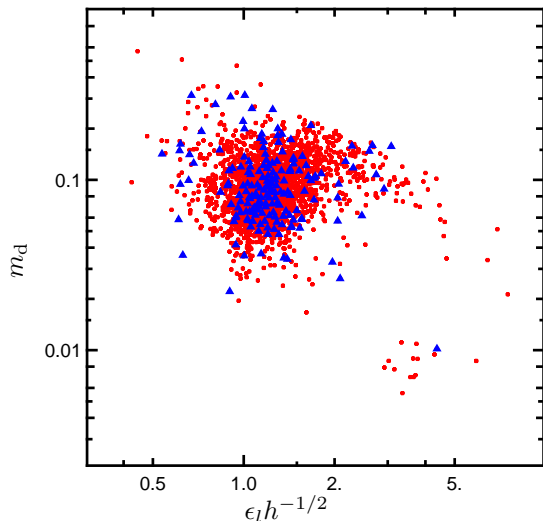


Figure 5. Shows $m_d = \chi a_m \Upsilon/h$ versus ϵ_l for the MF data, assuming that Υ_I is given by the crude upper limit $\Upsilon_I = (\epsilon_l/0.63)^2$. Barred galaxies are again plotted as triangles.

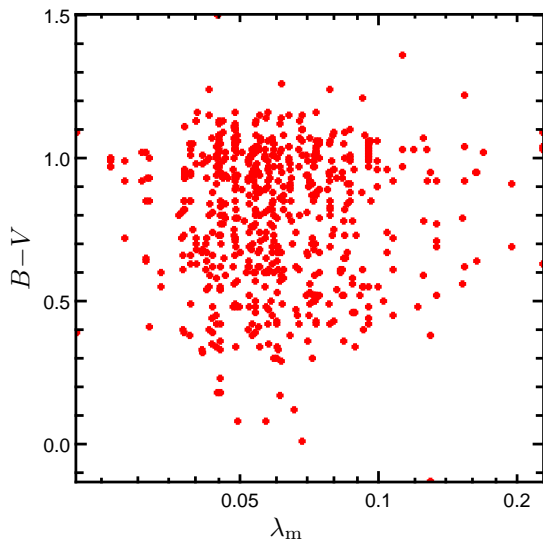


Figure 6. The MF galaxies which have $B-V$ colours in the ESO/Uppsala catalogue. There is a moderate scatter in $B-V$ but no trend with λ_m .

face brightness (corresponding to 23.5mag/arcsec^2). There is also a distance dependent component, selecting galaxies with a range of sizes which depends on their distance. To check that the selection function does not severely affect our results we constructed Monte-Carlo samples using the model in Section 2.2 and applied the selection function to them. The selection process reduced the apparent width of the λ distribution; the best fit to the data came from a distribution with $\sigma_\lambda \approx 0.4$. The values of χ and m_d (see below) are derived from $\bar{\lambda}$ and are little affected. One feature of the surface brightness threshold is that it tends to cut off the low-luminosity (low- v_m) galaxies in the Tully-Fisher relation, reducing the slope from the theoretical value (3) closer to that observed (≈ 2.5 in the MF sample).

4.3 Baryon fractions

Once χ is fixed, a_m can be estimated for each galaxy using equation (16). Restricting to those galaxies with $v_m > 100\text{km s}^{-1}$ we find that

$$\langle a_m \rangle = 0.47. \quad (21)$$

From equations (13) and (21) we have the total mass-to-light ratio in the I -band:

$$\langle M_h/L_I \rangle = \frac{1}{\chi \langle a_m \rangle} = 43h. \quad (22)$$

The observed mean luminosity of the Universe derived from recent redshift surveys of galaxies gives a critical mass-to-light ratio $(M/L) \approx 1500h(M/L)_\odot$ to close the universe (see e.g. Lin et al. 1996). Thus the mass associated with individual galactic halos gives $\Omega_{\text{gal}} = 43h/1500h \sim 0.03$, which is a small fraction of the total mass in the universe.

Using equations (13) and (21)

$$\langle m_d \rangle = 0.086 \frac{\Upsilon_I}{3.56h}. \quad (23)$$

The result is shown as a scatter plot in Figure 5 using the crude upper limit $\Upsilon_I = (\epsilon_l/0.63)^2$. The gas fraction obtained for X-ray clusters is $f_{\text{gas}} \sim 0.06h^{-3/2}$ (e.g. Evrard 1997). This fraction is usually considered to be equal to the mean value for the whole Universe (e.g. White *et al.* 1993), and therefore should be at least as large as that in galaxies. Equation (23) together with the gas fraction in clusters thus imply that

$$\langle \Upsilon_I \rangle \lesssim 2.48 h^{-1/2}. \quad (24)$$

which is a new upper limit independent of that derived in Section 4.1. Clearly, the observational constraint on the fraction of baryons in galactic halos has important implications for the formation of galactic disks.

5 DISCUSSION

5.1 Independent determinations of Υ

The disk mass-to-light ratios we derive in Section 4.1 are formally upper limits, and based only on rotation curve data. Thus they are consistent with mass-to-light ratios derived by other authors using the maximum disk hypothesis (Carignan & Freeman 1985, Palunas & Williams 1998).

Limits on the mass-to-light ratio of the Galactic disk in the solar neighbourhood can be derived from a combination of kinematic measurements and star counts. Kuijken & Gilmore (1989) derive a local surface mass density in the disk of $40M_\odot/\text{pc}^2$, and star counts give a V -band luminosity density of $15L_\odot/\text{pc}^2$ (Gould, Bahcall & Flynn 1996). Dividing mass by light we obtain $\Upsilon_V = 2.67$, and thus $\Upsilon_I \approx 1.9$ (assuming $V - I = 1.0$). This number is independent of h , but is comparable with the median maximum-disk value for the MF galaxies derived in Section 4.1 for $h \gtrsim 0.5$.

Mass-to-light ratios can also be derived from pure stellar population synthesis arguments, although there is always some uncertainty arising from the poorly known initial mass function (IMF), particularly from the low-mass cut-off in the IMF. A few stellar population models are available (e.g., Bertelli et al 1994; Bruzual & Charlot 1993; Worthey

1994). For a Salpeter IMF, the mass-to-light ratio derived by various authors appear to agree within an accuracy of 25% (Charlot, Worthey & Bressan 1996). The predicted Υ_I depends on the metallicity and age of the stellar population. For a stellar population with age between 5-12 Gyr and with a solar metallicity, Υ_I is between 0.9-1.8 for a constant star formation rate (cf Table 3 in de Jong 1996). For an exponential star formation law, the mass-to-light ratio is about 20% higher. The predicted values are in good agreement with the values derived in this paper. In the comparison, we have neglected the uncertainty due to dust, since the Tully-Fisher studies already attempt to correct for its effect. It has been argued (de Jong 1996) that dust reddening probably plays a minor role in the colour gradients in disk galaxies. Nevertheless, the dust correction remains a nuisance in these comparisons.

The mass-to-light ratio of extragalactic disks can also be measured directly from kinematic studies such as that described by Bottema (1993). The measurement of Υ relies on the relation between vertical velocity dispersion σ_z , surface density Σ and vertical scale height z_0 . Essentially, the larger the value of Σ , the hotter a disk has to be at constant z_0 . Using a small sample of very bright galaxies, Bottema (1997) derives a value of $\Upsilon_I = (1.7 \pm 0.5)h$, which is consistent with the upper limits we derived in Sections 4.1 and 4.3. It is important to extend the range of data analysed by Bottema (1997). This requires a good HI rotation curve for each galaxy, and high quality spectroscopy at least along the major axis of the galaxy. Ideally one would choose the brightest members of a large pre-defined sample (such as that of Mathewson & Ford 1996) and follow them up with a high spatial resolution spectrograph. Kinematic information in more than one dimension is also advantageous since it removes some of the uncertainties in the deprojection of the velocity ellipsoid. A number of two dimensional spectrographs are due to come on line shortly, and these may be well suited to the problem. The biggest uncertainty in the determination of Υ_I will remain that associated with the value of z_0 . Efforts should therefore be made to analyse as many edge on galaxies as possible to try to improve on existing determinations of the distribution of z_0/R_d (e.g. Barteldrees & Dettmar 1994).

5.2 Uncertainties in the results

The constant χ in equation (10) might in principle have been different owing to angular momentum loss. The fact that the derived value is close to the one expected in the disk formation model implies that the gas should not have lost much angular momentum during disk formation. This conclusion was also reached by Fall & Efstathiou (1980) and MMW based on the observed disk scale lengths of local galaxies. We confirmed this using our Monte-Carlo simulations: decreasing the value of χ led to disks with smaller R_d and larger μ at fixed v_m compared with the MF sample (L_d is fixed by the Tully-Fisher relation).

According to MMW, when realistic halo profiles are used and disk self-gravity included, the factor of $1/\sqrt{2}$ in equation (9) and the constant χ in equation (10) should in principle be replaced by quantities that depend on the spin parameter and concentration of galactic halos. The details of these dependences are uncertain, because they require ac-

curate knowledge on halo density profiles, gas settling processes and star formation feedback. To derive observational constraints on these details of disk formation requires detailed decompositions of individual galaxies into different components as well as accurate measurements of disk rotation curves. Such analysis is not possible with the data set used here.

As discussed in Section 4.1, the limit on the disk mass-to-light ratio was derived assuming that Υ_I is independent of μ_0 (or of λ_m , see Figure 1). This assumption is, as we argued, consistent with the observational data and with independent measurements of Υ_I (cf. Figure 6). Since the Tully-Fisher amplitude A derived from the data is quite independent of μ_0 for the majority of galaxies (cf. Figure 2), any trend in Υ_I with μ_0 has to be compensated by a similar trend in m_d . This would happen if disks with lower surface brightness contain larger amount of gas but have a lower star formation efficiency. Such a trend is suggested by the observations of McGaugh & de Blok (1997) where gas fraction in low surface-brightness disks is compared with that in high surface-brightness disks. However, for most of the galaxies in the MF sample, disk masses are expected to be dominated by stars rather by gas, and so the trend in the gas fraction with surface brightness should not induce a significant trend in the disk mass-to-light ratio.

5.3 Barred galaxies

It is well known that isolated disks are violently unstable. Since disks in halos with lower spin parameters are more compact and more self-gravitating, they are more prone to global instabilities. One obvious possibility is that globally unstable disks turn into barred galaxies. If so one might expect that barred galaxies to have systematically smaller λ_m and larger μ_0 . No such trend is seen in Figure 1 where barred galaxies (triangles) seem to be randomly drawn from the galaxy population. Two possibilities occur to us. First, if Υ is universal, then global instabilities in disk galaxies must be switched off by some mechanism which is independent of μ_0 . Such a mechanism might involve central mass concentrations (Toomre 1981) which stabilise a disk by interfering with transmission of density waves through the centre (Sellwood & Moore 1998). Second, if Υ depends on μ_0 , then it must do so in such a way as to make all galaxies equally susceptible to bar formation. Bars could then be formed by interactions between galaxies (Noguchi 1996), or between galaxies and their dark matter halos. (N.B. the Tully-Fisher relation then requires that m_d depends on μ_0 .)

ACKNOWLEDGMENTS

We are grateful to Simon White for helpful discussions. This project is partly supported by the ‘‘Sonderforschungsbereich 375-95 f ur Astro-Teilchenphysik’’ of the Deutsche Forschungsgemeinschaft.

REFERENCES

- Bertelli G., Bressan A., Chiosi C., Fagotto F. & Nasi E., 1994, AA Supp., 106, 275

- Barteldrees A. & Dettmar R.-J., 1994, *AA Supp.*, 103, 475
 Bottema R., 1993, *A&A*, 275, 16
 Bottema R., 1997, preprint (astro-ph/9706230)
 Bruzual G. A., Charlot S., 1993, *ApJ*, 405, 538
 Carignan C. & Freeman K.C., 1985, *ApJ*, 294, 494
 Charlot S., Worthey S. & Bressan A., 1996, *ApJ*, 457, 625
 Cole S. & Lacey C., 1996, *MNRAS*, 281, 716
 Courteau S., 1996, *ApJS*, 103, 363
 Courteau S., 1997, *ApJS*, 000, in press
 Courteau S. & Rix H.-W., 1997, preprint (astro-ph/9707290)
 Dalcanton J.J., Spergel D.N. & Summers F.J., 1997, *ApJ*, 482, 659
 de Jong R.S., 1996, *A&A*, 313, 377
 Evrard A.E., 1997, preprint (astro-ph/9701148)
 Fall S.M. & Estafthiou G., 1980, *MNRAS*, 193, 189
 Freeman K.C., 1970, *ApJ*, 160, 811
 Gould A., Bahcall J.N. & Flynn C., 1996, *ApJ*, 465, 759
 Giovanelli R., Haynes M.P., da Costa L.N., Freudling W., Salzer J.J. & Wegner G., 1997, preprint (astro-ph/9612072)
 Kennicutt R.C., Jr., 1989, *ApJ*, 344, 685
 Kuijken K. & Gilmore G., 1989, *MNRAS*, 239, 605
 Lauberts A., 1982, *The ESO/Uppsala Survey of the ESO(B) Atlases*, European Southern Observatory.
 Mathewson D.S. & Ford L., 1996, *ApJS*, 107, 97 (MF)
 McGaugh S.S. & de Blok W.J.G., 1997, *ApJ*, 481, 689
 Mo, H.J., Mao, S. & White S.D.M., 1998, *MNRAS*, 295, 319 (MMW)
 Noguchi M., 1996, in *Barred Galaxies*, IAU Colloquium 157, San Francisco: ASP, p.339
 Palunas P., & Williams T.B., 1998, *ApJS*, 000, submitted
 Persic M. & Salucci P., 1991, *ApJ*, 285, 307
 Sellwood J.A., & Moore E.M., 1998, preprint (astro-ph/9807010)
 Shanks T., 1997, preprint (astro-ph/9702148)
 Steinmetz M. & Bartelmann M., 1995, *MNRAS*, 272, 570
 Toomre, A., 1981, in *Structure and Evolution of Normal Galaxies*, ed. Fall, S.M. & Lynden-Bell, D., (Cambridge: CUP), p. 111.
 Tully R.B. & Fisher J.R., 1977, *A&A*, 54, 661
 Warren, M.S., Quinn, P.J., Salmon, D.N. & Zurek, W.H., 1992, *ApJ*, 376, 51
 White S.D.M. & Rees M.J., 1978, *MNRAS*, 183, 341
 White S.D.M., Navarro J.F., Evrard A.E., Frenk C.S., 1993, *Nature*, 366, 429
 Worthey G., 1994, *ApJS*, 95, 107

APPENDIX

Here we describe how values of R_d , μ_0 and L were derived from the published quantities of Mathewson & Ford (1996). The published data list total magnitudes, and face-on corrected isophotal quantities: average surface brightness ($\bar{\mu}$) and isophotal diameter (R) at μ corresponding to 23.5mag/arcsec². Assuming an exponential disk we have a surface brightness profile

$$\mu(R) = \mu_0 \exp(-\alpha), \quad \alpha \equiv \frac{R}{R_d}, \quad (25)$$

and

$$L(R) = L_d (1 - \exp(-\alpha)(\alpha + 1)). \quad (26)$$

From equation (26) the average surface brightness inside radius R is

$$\bar{\mu} = \frac{L(R)}{\pi R^2} = \frac{2\mu_0}{\alpha^2} (1 - \exp(-\alpha)(\alpha + 1)), \quad (27)$$

where we have used $L_d = 2\pi\mu_0 R_d^2$. Combining equations (26) and (27) we obtain

$$\frac{\bar{\mu}}{\mu} = \frac{\exp(\alpha) - (\alpha + 1)}{\alpha^2}. \quad (28)$$

Given $\bar{\mu}/\mu$ we can solve equation (28) numerically to find α . Then we have $R_d = R/\alpha$, and $\mu_0 = \mu \exp(\alpha)$.

This paper has been produced using the Royal Astronomical Society/Blackwell Science L^AT_EX style file.